

Triply Interpenetrated Structure of $\{Mn^{II}(L)_2[Ag^{I}(CN)_2]_2\}$-$\{Mn^{II}(H_2O)_2[Ag^{I}(CN)_2]_2\}$ (L = 4-CNpy or py-4-aldoxime)

Takeshi Kawasaki,[1] Chihiro Kachi-Terajima,[1] Toshiaki Saito,[2,3] and Takafumi Kitazawa*[1,2]

[1]Department of Chemistry, Faculty of Science, Toho University, 2-2-1 Miyama, Funabashi 274-8510

[2]Research Center for Materials with Integrated Properties, Toho University, Miyama, Funabashi 274-8510

[3]Department of Physics, Faculty of Science, Toho University, 2-2-1 Miyama, Funabashi 274-8510

Received July 5, 2007; E-mail: kitazawa@chem.sci.toho-u.ac.jp

Two novel 3D network coordination polymers $\{Mn(L)_2[Ag(CN)_2]_2\}\{Mn(H_2O)_2[Ag(CN)_2]_2\}$ (L = 4-CNpy (**1**) or py-4-aldoxime (**2**)) (4-CNpy = 4-cyanopyridine; py-4-aldoxime = pyridine-4-aldoxime) were synthesized and characterized by using single-crystal X-ray analysis and magnetic measurements. Both complexes have two distinct octahedral manganese atoms, Mn(1) and Mn(2), linked by a $[Ag(CN)_2]^-$ unit. The pyridine ring of two Ls coordinate at the apical positions of Mn(1). On the other hand, at the apical positions of Mn(2), two H_2O are coordinated. The apical axis of Mn(1) is not parallel to the apical axis of Mn(2). Therefore, $\{Mn[Ag(CN)_2]_2\}$ networks in **1** and **2** are distorted and form three-dimensional (3D) frameworks. There are large channels in the 3D networks; however, triple interpenetration was found in **1** and **2**. From the temperature dependence of magnetic susceptibility, there is very weak antiferromagnetic interaction between the Mn atoms bridged by a $[Ag(CN)_2]^-$ unit in **1** and **2**.

Inorganic coordination polymers self-assembled from simple building blocks are currently drawing a great deal of attention due to their intriguing network topologies and their potential uses in molecular devices, non-linear optics, porous materials, and other applications. Polycyanometalates are useful building blocks for various kinds of coordination polymers with interesting properties, such as clathrate host,[1] spin-crossover phenomena,[2–7] and molecular magnet.[8] Among the synthetic strategies for cyano-bridged coordination polymers, linear dicyanometalates $[M^{I}(CN)_2]^-$ (M = Ag and Au) have been used as building blocks, because they can bridge coordination centers through the nitrogen atoms of the cyano groups. One example of a coordination polymer built with a dicyanometalate is $\{Cd(py)_2[Ag(CN)_2]_2\}$ (py = pyridine), which has been reported by Soma and Iwamoto.[1a] It has a 2D $\{Cd[Ag(CN)_2]_2\}$ network structure, including the large rhombus $\{Cd_4[Ag(CN)_2]_4\}$. We have reported $\{Fe(py)_2[Ag(CN)_2]_2\}$, which undergoes a two-step spin-crossover phenomenon.[3] This complex is isostructural to $\{Cd(py)_2[Ag(CN)_2]_2\}$. In $\{M'(pz)[M(CN)_2]_2\}$ (pz = pyrazine) (M′ = Fe, M = Ag[4] and M′ = Cu, M = Au[5]), the complexes possess an interpenetrated 3D "jungle gym" network structure involving the pz bridge between the M′ metals in the 2D $\{M'[M(CN)_2]_2\}$ layers. $\{Fe(3\text{-}CNpy)_2[Ag(CN)_2]_2\}\cdot 2/3H_2O$[6] and $\{Fe(pmd)(H_2O)[M(CN)_2]_2\}$ (M = Ag or Au)[7] (pmd = pyrimidine) have 3D $\{Fe[M(CN)_2]_2\}$ networks with the apical ligands on the iron atoms, which correspond to an expanded version of the prototypal NbO and $CdSO_4$ nets, respectively.

Complexes with flexible $[M(CN)_2]$ units have been reported. In $\{M'(4,4'\text{-bpy})_2[Ag(CN)_2]_2\}$ (M′ = Mn,[9] Fe,[4] and Cd[10]) and $\{Fe(bpe)_2[Ag(CN)_2]_2\}$ (4,4′-bpy = 4,4′-bipyridyl; bpe = *trans*-bis(4-pyridyl)ethylene),[4] 3D doubly interpenetrating frameworks are built by stacking $\{M[Ag(CN)_2]_2\}$ layer networks, and 4,4′-bipyridyl ligands bridge from a M atom in one network, which penetrate through the $\{M_4[Ag(CN)_2]_4\}$ meshes of the adjacent networks, to two Ag atoms in the next networks. The Ag atoms in these complexes are three-coordinate, and consequently, the C–Ag–C moieties are bent. $\{Cd(4\text{-}Mepy)_2[Ag(CN)_2]_2\}\cdot 4\text{-}Mepy$[1] has a "stationary wave" structure, although the Ag atom is 2-coordinate. In $\{Mn(NITppy)_2[Ag(CN)_2]_2\}$ (NITppy = 2-(4-pyridyl)-4,4,5,5-tetramethylimidazoline-1-oxyl-3-oxide),[11] two $[Ag(CN)_2]^-$ ions bridge two Mn atoms.

Another interesting feature of some of these silver and gold compounds is the metallophilic interactions.[1,4–7,10,12,13] Metallophilicity is a closed-shell intermolecular interaction between silver(I) or gold(I) atoms.[14] The interactions are comparable to hydrogen bonds.[13,14] In the case of silver, the attraction has been called an argentophilic interaction.

The octahedral Mn^{II}–$[Ag(CN)_2]$ complexes are isostructural to Fe^{II}–$[Ag(CN)_2]$ complexes. Some octahedral Fe^{II}–$[Ag(CN)_2]$ compounds, such as $\{Fe(py)_2[Ag(CN)_2]_2\}$,[3] exhibit spin-crossover phenomena. The crystal structures of octahedral Mn^{II}–$[Ag(CN)_2]$ compounds are similar to that of Fe^{II}–$[Ag(CN)_2]$.[4,9] In this work, we report the synthesis, crystal structure, and magnetic properties of novel bimetallic 3D triply interpenetrated coordination polymers with the formula $\{Mn(L)_2[Ag(CN)_2]_2\}\{Mn(H_2O)_2[Ag(CN)_2]_2\}$ (L = 4-CNpy (**1**) or py-4-aldoxime (**2**)) (4-CNpy = 4-cyanopyridine; py-4-aldoxime = pyridine-4-aldoxime).

Experimental

Synthesis. To an aqueous solution (15 mL) containing $MnCl_2\cdot 4H_2O$ (0.14 g, 0.7 mmol) and L (L = 4-CNpy or py-4-aldoxime) (1.4 mmol) was added an aqueous solution of $K[Ag(CN)_2]$ (0.28 g, 1.4 mmol). The aqueous solution was kept standing

Published on the web February 12, 2008; doi:10.1246/bcsj.81.268

Table 1. Crystal Data

Crystal data	**1**	**2**
Empirical formula	$C_{20}H_{12}Ag_4Mn_2N_{12}O_2$	$C_{20}H_{16}Ag_4Mn_2N_{12}O_4$
FW	993.78	1029.81
Temperature/K	273	298
Crystal system	Orthorhombic	Monoclinic
Space group	*Pnma*	*C*2/*c*
a/Å	7.5831(4)	31.4924(18)
b/Å	31.0864(17)	13.2986(8)
c/Å	13.7989(7)	7.4416(4)
β/°	–	100.2260(10)
V/Å^3	3252.8(3)	3067.1(3)
Z	4	4
d(calc.)/Mg m^{-3}	2.029	2.230
Absorption Coefficient/mm^{-1}	3.150	3.350
F(000)	1880	1960
Crystal size/mm^{-3}	0.27 × 0.17 × 0.10	0.30 × 0.10 × 0.06
Reflections collected	22875	11238
Independent	4116	3806
Reflections	[*R*(int) = 0.0273]	[*R*(int) = 0.0206]
GOF on F^2	1.058	1.118
*R*1[a], *wR*2[b]	0.0250, 0.0641	0.0530, 0.1285
Largest diff. peak and hole/e.Å^{-3}	0.823 and −0.751	2.691 and −1.399

a) $R1 = (\Sigma||F_o| - |F_c||)/\Sigma|F_o|$. b) $wR2 = \{\Sigma w(|F_o| - |F_c|)^2/\Sigma w|F_o|^2\}^{1/2}$.

Table 2. Selected Bond Lengths and Angles

1	**2**
Bond lengths/Å	
Mn(1)–N(1) 2.213(2)	Mn(1)–N(1) 2.216(5)
Mn(1)–N(3) 2.196(2)	Mn(1)–N(3) 2.216(5)
Mn(1)–N(5) 2.310(2)	Mn(1)–N(5) 2.294(5)
Mn(2)–N(2) 2.235(2)	Mn(2)–N(2) 2.203(5)
Mn(2)–N(4) 2.186(2)	Mn(2)–N(4) 2.196(5)
Mn(2)–O(1) 2.196(3)	Mn(2)–O(1) 2.211(6)
Mn(2)–O(2) 2.221(3)	Mn(2)–O(2) 2.260(7)
Ag(1)–C(3) 2.053(2)	Ag(1)–C(3) 2.059(6)
Ag(1)–C(4) 2.053(3)	Ag(1)–C(4) 2.066(6)
Ag(2)–C(1) 2.057(2)	Ag(2)–C(1) 2.066(6)
Ag(2)–C(2) 2.058(2)	Ag(2)–C(2) 2.057(6)
Bond angles/°	
N(1)–Mn(1)–N(3) 87.82(8)	N(1)–Mn(1)–N(3) 88.9(2)
N(1)–Mn(1)–N(5) 89.57(8)	N(1)–Mn(1)–N(5) 87.90(19)
N(3)–Mn(1)–N(5) 88.96(8)	N(3)–Mn(1)–N(5) 89.06(19)
N(2)–Mn(2)–N(4) 85.21(9)	N(2)–Mn(2)–N(4) 87.3(2)
O(1)–Mn(2)–O(2) 165.36(16)	O(1)–Mn(2)–O(2) 180.000(1)
O(1)–Mn(2)–N(2) 88.46(9)	O(1)–Mn(2)–N(2) 94.05(16)
O(2)–Mn(2)–N(2) 82.05(10)	O(2)–Mn(2)–N(2) 85.95(16)
O(1)–Mn(2)–N(4) 97.15(10)	O(1)–Mn(2)–N(4) 85.07(15)
O(2)–Mn(2)–N(4) 93.17(12)	O(2)–Mn(2)–N(4) 94.93(15)
C(3)–Ag(1)–C(4) 173.58(11)	C(3)–Ag(1)–C(4) 173.1(3)
C(1)–Ag(2)–C(2) 174.77(10)	C(1)–Ag(2)–C(2) 173.1(3)

at 5 °C in a refrigerator. Pale yellow crystals were obtained after 24 h. **1**: Elemental Analysis: Found: C, 23.53; H, 1.47; N, 16.27%. Calculated for $C_{20}H_{12}Ag_4Mn_2N_{12}O_2$: C, 24.17; H, 1.22; N, 16.92%. IR (nujol method, cm^{-1}): 2248 (ν_{CN} (4-CNpy)), 2156 (ν_{CN} (CN)). **2**: Elemental Analysis: Found: C, 23.32; H, 1.66; N, 15.90%. Calculated for $C_{20}H_{16}Ag_4Mn_2N_{12}O_4$: C, 23.32; H, 1.56; N, 16.32%; IR (nujol method, cm^{-1}): 2152 (ν_{CN}).

Structure Determination. Crystal structures of the two complexes were determined using a BRUKER APEX SMART CCD area-detector diffractometer with monochromeated Mo Kα radiation (λ = 0.71073 Å). The diffraction data were treated using SMART and SAINT, and absorption correction was performed using SADABS.[15] The structures were solved by using direct methods with SHELXTL.[16] All non-hydrogen atoms were refined anisotropically, and the hydrogen atoms were generated geometrically. In the structure determination of **2**, C(7)–C(10) and C(10)–N(6) bond lengths were refined using DFIX command. The crystal data of **1** and **2** are listed in Table 1.

Crystallographic data have been deposited with Cambridge Crystallographic Data Centre: Deposition numbers CCDC-665141 for compound No. **1** and CCDC-665142 for compound No. **2**. Copies of the data can be obtained free of charge via http://www.ccdc.cam.ac.uk/conts/retrieving.html (or from the Cambridge Crystallographic Data Centre, 12, Union Road, Cambridge, CB2 1EZ, UK; Fax: +44 1223 336033; e-mail: deposit@ccdc.cam.ac.uk).

Magnetic Measurement. Measurements of the temperature dependence of the magnetic susceptibility of the two complexes in the temperature range of 2–300 K with a cooling and heating rate of 0.5 K min^{-1} in a 1 kOe field and the field-dependent magnetization of **1** at 2 K were measured on a MPMS-XL Quantum Design SQUID magnetometer.

Results and Discussion

Synthesis and IR Spectra. The reaction of an aqueous solution of $MnCl_2 \cdot 4H_2O$ containing two equivalents of pyridine-derivative ligand (L = 4-CNpy or py-4-aldoxime) with an aqueous solution of two equivalents of $K[Ag(CN)_2]$ afforded crystals of the 3D cyano-bridged complex $\{Mn(L)_2[Ag(CN)_2]_2\}\{Mn(H_2O)_2[Ag(CN)_2]_2\}$ (L = 4-CNpy (**1**) or py-4-aldoxime (**2**)).

Bridging or terminal cyano groups can usually be differentiated by the positions of the corresponding IR ν_{CN} stretching absorption bands, because bridging cyano ligands show peaks at higher wavenumbers. The solid infrared spectra of **1** and **2** had ν_{CN} bands at 2156 cm^{-1} for **1** and 2152 cm^{-1} for **2**, which are both at higher wavenumbers than that of free $[Ag(CN)_2]^-$ (2135 cm^{-1}), at room temperature. This suggests that both of the cyano groups of $[Ag(CN)_2]^-$ act as bridging ligands.

Crystal Structure. Complexes **1** and **2** crystallized in the centrosymmetric space groups *Pnma* and *C*2/*c*, respectively. Selected bond lengths and angles of **1** and **2** are listed in Table 2, and three-dimensional frameworks of **1** and **2** are shown in Fig. 1. In complex **1**, the $[Ag(CN)_2]^-$ units are almost linear (Fig. 2a). There are two types of manganese ions (Mn(1) and Mn(2)). Mn(1) lies on an inversion center with a N_6 coordination sphere. Mn(2) has a N_4O_2 coordination sphere and lies on a mirror plane involving O(1) and O(2). Four nitrogen atoms from CN^- groups are coordinated to both Mn atoms in the equatorial positions. The pyridyl N atoms from two 4-CNpy ligands coordinate in the apical positions of Mn(1) (Fig. 2a). The Mn(1)–N_{py} bond lengths are longer than the

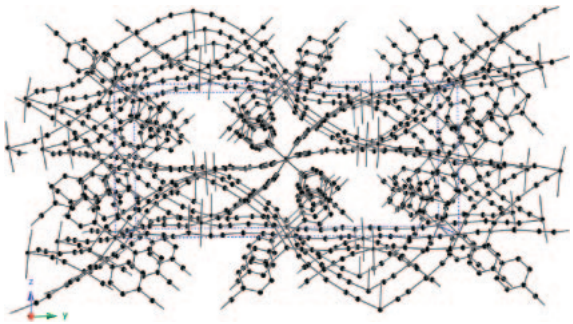

(a)

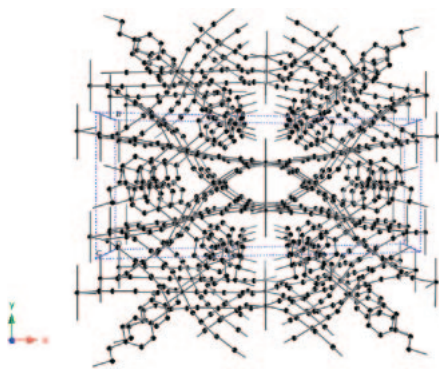

(b)

Fig. 1. Crystal structures of **1** (a) and **2** (b).

Mn(1)–N_{CN} bond lengths. On the other hand, two H_2O (O(1) and O(2)) coordinate in the apical positions of Mn(2) (Fig. 2a). The Mn(2)–O bond lengths are almost equal to the Mn(2)–N_{CN} bond lengths. The Mn(2)–O(1) bond length is shorter than the Mn(2)–O(2) bond distance. The O(1)–Mn(2)–O(2) angle is 165.4(2)°. Each $[Ag(CN)_2]^-$ group bridges between Mn(1) and Mn(2), defining the edges of a large $\{Mn(1)_2Mn(2)_2[Ag(CN)_2]_4\}$ mesh. The Mn···Mn distances in the Mn(1)–NC–Ag(1)–CN–Mn(2) edge and Mn(1)–NC–Ag(2)–CN–Mn(2) edge are 10.644 and 10.513 Å, respectively. The length of the hydrogen bond between N(6) of cyano group in 4-CNpy and O(1) is 2.963(4) Å. Due to N(6)···O(1) hydrogen bonds, the apical axis of Mn(1) is not parallel to the apical axis of Mn(2). Consequently, the $\{Mn(1)_2Mn(2)_2[Ag(CN)_2]_4\}$ mesh is bent, and the mesh structure has a boat-form (Fig. 2b). Thus, there are large channels in the 3D "stationary wave" $\{Mn[Ag(CN)_2]_2\}$ networks of **1** (Fig. 2c); however, there is triple interpenetration, as shown in Fig. 2d. The closest approach between networks corresponds to argentophilic Ag(1)···Ag(2) interactions, which define zigzag-chain Ag arrangements (Fig. 2d). The Ag(1)···Ag(2) distances are 3.240 and 3.341 Å.

The coordination environment of the Mn ions and Ag atoms in complex **2** are similar to those of **1** (Fig. 3a). The Mn(2)–O(2) bond is longer than the Mn(2)–O(1) bond. The O(1)–Mn(2)–O(2) angle is linear. The Mn···Mn distances in the Mn(1)–NC–Ag(1)–CN–Mn(2) and Mn(1)–NC–Ag(2)–CN–Mn(2) edges are 10.357 and 10.496 Å, respectively. Hydrogen bonds exist between O(3) (OH of py-4-aldoxime) and O(2)

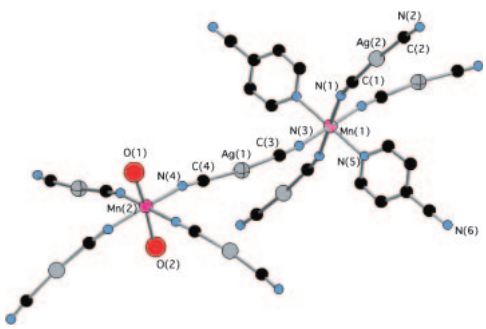

(a)

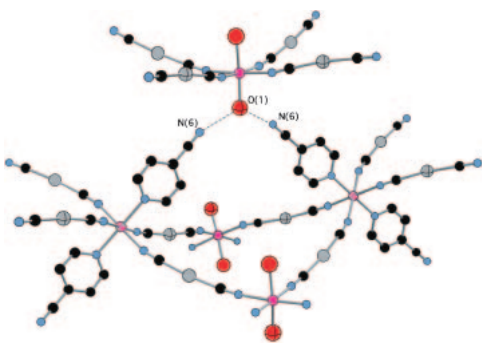

(b)

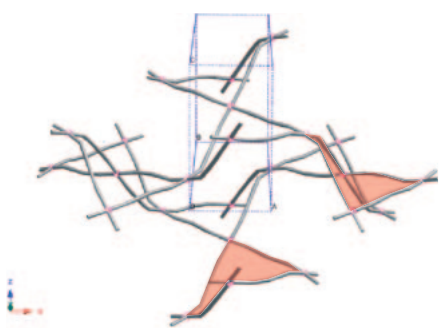

(c)

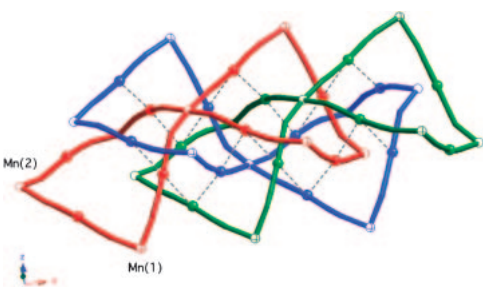

(d)

Fig. 2. (a) Coordination structure of the Mn and Ag ions in **1**. (b) Hydrogen bonds of **1**. Due to hydrogen bonding, the $\{Mn(1)_2Mn(2)_2[Ag(CN)_2]_4\}$ mesh structure is boat-form. (c) Network structure of **1**. Apical ligands are omitted for clarity. (d) Triple interpenetrated $\{Mn[Ag(CN)_2]_2\}$ networks of **1** (red, blue, and green) and argentophilic interactions (black line) among the networks.

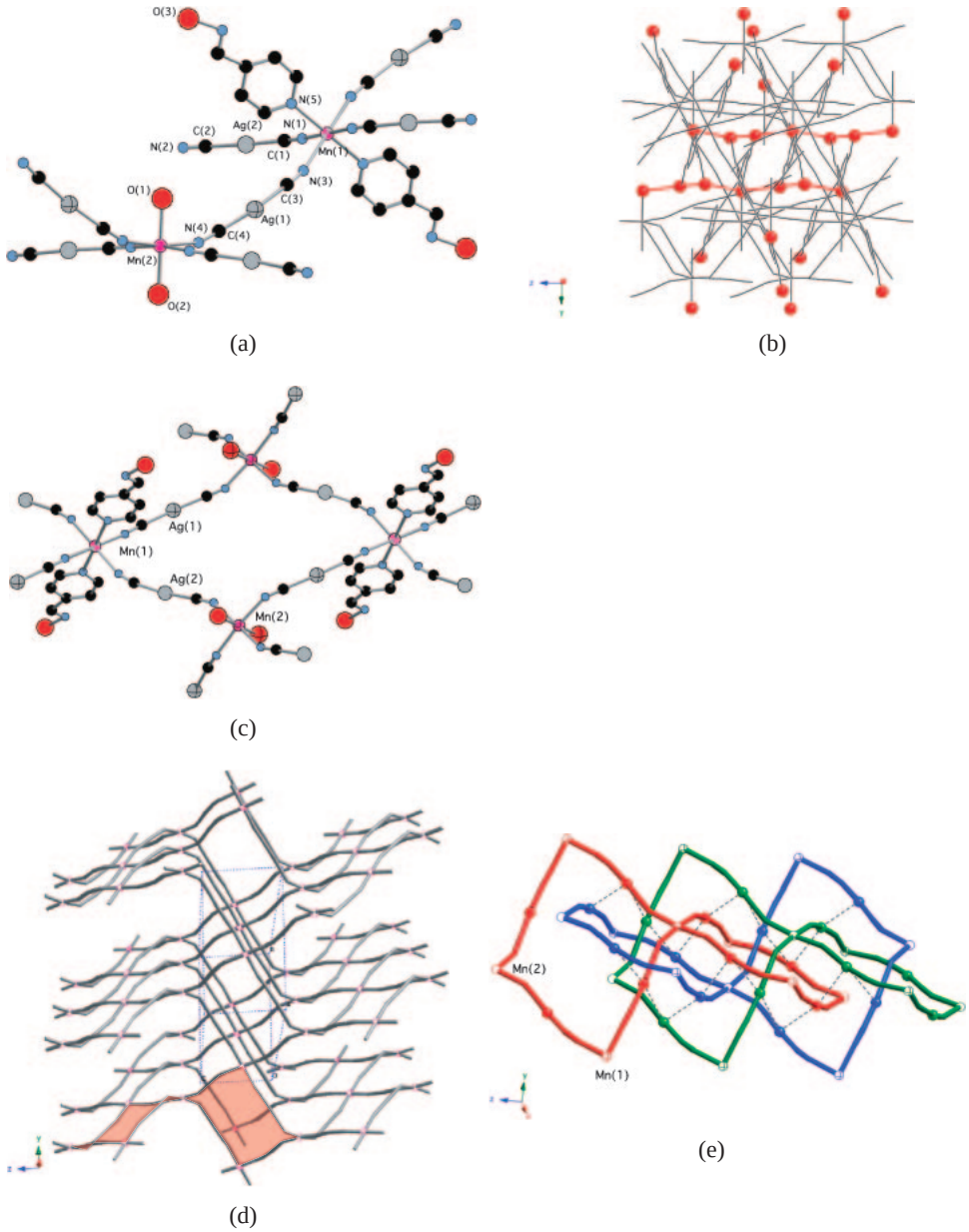

Fig. 3. (a) Coordination structure of the Mn atoms and Ag ions in **2**. (b) Chain formed by O(2)···O(3) and O(3)···O(3) hydrogen bonds in **2**. (c) $\{Mn(1)_2Mn(2)_2[Ag(CN)_2]_4\}$ rhombus. (d) Network structure of **2**. Apical ligands are omitted for clarity. (e) Triple interpenetrated $\{Mn[Ag(CN)_2]_2\}$ networks of **2** (red, blue, and green) and argentophilic interactions (black line) among the networks.

(H_2O-coordinated Mn(2)), and between O(3) and O(3), of which the distances are 2.936(7) and 2.83(2) Å, respectively. The 1D chains are constructed from these hydrogen bonds (Fig. 3b). The large $\{Mn(1)_2Mn(2)_2[Ag(CN)_2]_4\}$ moiety has a chair structure (Fig. 3c). The $\{Mn[Ag(CN)_2]_2\}$ networks are triply interpenetrated, and the Ag(1)···Ag(2) distances are 3.130 and 3.308 Å between the networks (Fig. 3e).

Magnetic Property. χ_M versus T and $\chi_M T$ versus T plots for **1** and **2** are shown in Fig. 4. For both complexes, the $\chi_M T$ values were nearly constant in the range of 60–300 K; however, they decreased as the temperature was lowered less than 60 K. The values of μ_{eff} ($\mu_{eff} = 2.828\sqrt{(\chi_M T)}$) of **1** and **2** per one Mn atom at 300 K were 5.74 and 5.81 μ_B, respectively. These values are slightly smaller than 5.92 ($=g\sqrt{(S(S+1))}$, $g = 2$, $S = 5/2$) that of a pure spin only system, whereas the values are similar to the μ_{eff} value at 300 K of $\{KMn[Ag(CN)_2]_3(H_2O)\}$ (5.76 μ_B).[9] The magnetic values could be fitted with the Curie–Weiss equation $\chi_M = C/(T-\theta)$, where $C = 8.28$ emu K mol^{-1} and $\theta = -0.29$ K for **1** and $C = 8.45$ emu K mol^{-1} and $\theta = -0.36$ K for **2**. These slightly negative θ values seem consistent with very weak antiferromagnetic interaction between two Mn^{II} atoms with $S = 5/2$ spins bridged by a $[Ag(CN)_2]^-$ unit. The field dependence of the magnetization of **1** at 2 K was below the Brillouin function curve and reached a value of 9.32 $N\beta$ at 50 kOe, as expected for weak antiferromagnetic interactions between two Mn^{II} atoms (Fig. 5). Similar magnetic behavior has been reported for $[Mn^{II}{}_2(\text{macrocycle})_2(H_2O)][Mo^{IV}(CN)_8]\cdot 5H_2O$ (macrocycle =

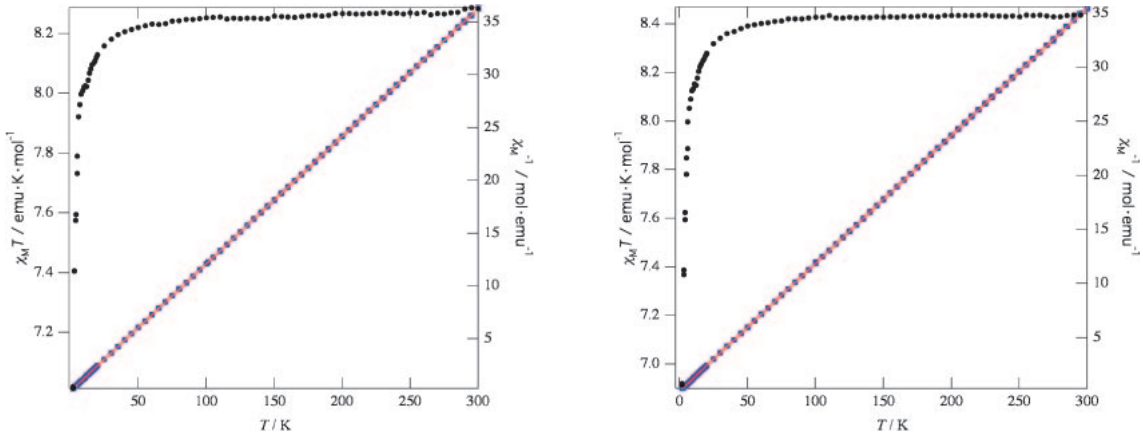

Fig. 4. Magnetic properties of **1** (a) and **2** (b). $\chi_M T$ vs. T (black points) and χ_M^{-1} vs. T (blue points) plot from 0 to 300 K. The red lines show the best-fit calculation of Curie–Weiss law.

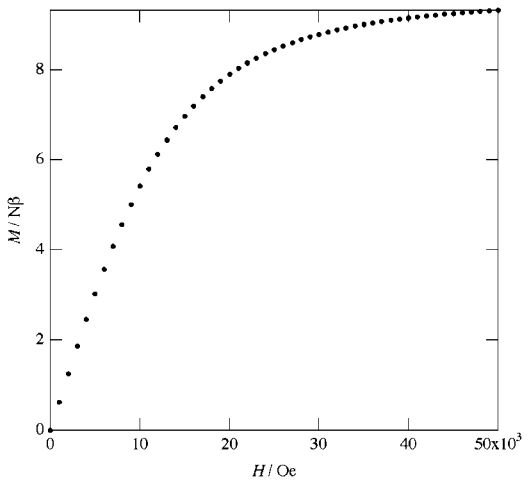

Fig. 5. Field-dependent isothermal magnetization for **1** at 2 K.

2,13-dimethyl-3,6,9,12,18-pentaazabicyclo-[12.3.1]octadeca-l(18),2,12,14,16-pentanene).[17] The decrease in the values of $\chi_M T$ at low temperatures is characteristic of weak antiferromagnetic coupling, but it may be also due to zero-field splitting (ZFS) effects of the sextuplet spin state of the Mn^{II} ions.[18–20] In general, for Mn^{II} ions, ZFS is small. Nevertheless, in **1** and **2**, ZFS may be important, because the octahedral geometries of the Mn^{II} ions in **1** and **2** are slightly distorted.

Conclusion

We synthesized new crystalline coordination polymers with the formula $\{Mn(L)_2[Ag(CN)_2]_2\}\{Mn(H_2O)_2[Ag(CN)_2]_2\}$ (L = 4-CNpy (**1**) or py-4-aldoxime (**2**)). In complex **1** and **2**, two distinct manganese atoms, Mn(1) and Mn(2), constitute the building blocks of these structures. $[Ag(CN)_2]^-$ bridges Mn(1) and Mn(2), defining the edges of a large $\{Mn(1)_2Mn(2)_2[Ag(CN)_2]_4\}$ mesh. Due to hydrogen bonding between L and H_2O, the apical axis of Mn(1) is not parallel to the apical axis of Mn(2). Thus, the quasi-linear bidentate $[Ag(CN)_2]^-$ bridges and the Mn atoms assemble to form a 3D $\{Mn[Ag(CN)_2]_2\}$ network. There are large channels in the 3D networks; however, triple interpenetration occurs in **1** and **2**. The attraction between networks corresponds to argentophilic interactions, which create Ag zigzag-chain arrangements. From the measurements of the temperature dependence of the magnetic susceptibility, very a weak antiferromagnetic interaction occurs between the Mn(1) and Mn(2) bridged by $[Ag(CN)_2]^-$ unit in **1** and **2**.

In many dicyanometalates complexes, $[M(CN)_2]^-$ (M = Ag and Au) behaves as a bridging ligand between metal atoms (e.g., Mn, Fe, Co, Cd, etc.) to form multi-dimensional structures, such as 1D chains,[11,12] 2D layers,[1,3,13] and 3D frameworks,[4–7,9,10] including **1** and **2** in this study. These fact suggest that structural control to from multi-dimensional structures involving –NC–M–CN– linkages between M′ atoms with the secondary ligands is delicate work and that the construction of supramolecular coordination structures with a large channel should give rise to unexpected crystal packing or inclusion structures that have not been observed previously. This work also shows that it may be possible to prepare analogous iron(II) compounds, which may have interesting magnetic properties, such as spin-crossover behavior and molecular magnetism. These new Mn^{II} compounds should be useful as crystalline model compounds for studying spin-crossover in analogous iron(II) compounds and for controlling coordination frameworks on the nanoscale level.

Supporting Information

Figures S1–S4 are in PDF format. This material is available free of charge on the Web at: http://www.csj.jp/journals/bcsj/.

References

1 a) T. Soma, T. Iwamoto, *J. Inclusion Phenom. Macrocyclic Chem.* **1996**, *26*, 161. b) T. Soma, T. Iwamoto, *Chem. Lett.* **1994**, 821.

2 T. Kitazawa, Y. Gomi, M. Takahashi, M. Takeda, M. Enomoto, A. Miyazaki, T. Enoki, *J. Mater. Chem.* **1996**, *6*, 119.

3 a) T. Kitazawa, T. Kawasaki, M. Takahashi, M. Takeda, KURRI-KR-106, **2004**, p. 1. b) J. A. Rodríguez-Velamazán, M. Castro, E. Palacios, R. Burriel, T. Kitazawa, T. Kawasaki, *J. Phys. Chem. B* **2007**, *111*, 1256.

4 V. Niel, M. C. Muñoz, A. B. Gaspar, A. Galet, G. Levchenko, J. A. Real, *Chem. Eur. J.* **2002**, *8*, 2446.

5 a) D. B. Leznoff, B.-Y. Xue, C. L. Stevens, A. Storr, R. C. Thompson, B. O. Patrick, *Polyhedron* **2001**, *20*, 1247. b) D. B. Leznoff, J. Lefebvre, *Gold Bull.* **2005**, *38*, 47.

6 A. Galet, V. Niel, M. C. Muñoz, J. A. Real, *J. Am. Chem. Soc.* **2003**, *125*, 14224.

7 V. Niel, A. L. Thompson, M. C. Muñoz, A. Galet, A. E. Goeta, J. A. Real, *Angew. Chem., Int. Ed.* **2003**, *42*, 3760.

8 a) Z. J. Zhong, H. Seino, Y. Mizobe, M. Hidai, A. Fujishima, S. Ohkoshi, K. Hashimoto, *J. Am. Chem. Soc.* **2000**, *122*, 2952. b) J. J. Sokol, A. G. Hee, J. R. Long, *J. Am. Chem. Soc.* **2002**, *124*, 7656.

9 W. Dong, Q.-L. Wang, S.-F. Si, D.-Z. Liao, Z.-H. Jiang, S.-P. Yan, P. Cheng, *Inorg. Chem. Commun.* **2003**, *6*, 873.

10 T. Soma, H. Yuge, T. Iwamoto, *Angew. Chem., Int. Ed. Engl.* **1994**, *33*, 1665.

11 I. Dasna, S. Golhen, L. Ouahab, N. Daro, J.-P. Sutter, *Polyhedron* **2001**, *20*, 1371.

12 I. P. Y. Shek, W.-Y. Wang, T.-C. Lau, *New J. Chem.* **2000**, *24*, 733.

13 E. Colacio, F. Lloret, R. Kivekäs, J. Ruiz, J. Suárez-Varela, M. R. Sundberg, *Chem. Commun.* **2002**, 592.

14 P. Pyykkö, *Chem. Rev.* **1997**, *97*, 597.

15 G. M. Sheldrick, *SADABS, Program for Empirical Absorption Correction for Area Detector Data*, University of Göttingen, Göttingen, Germany, **1996**.

16 G. M. Sheldrick, *SHELXL, Program for the Solution of Crystal Structures*, University of Göttingen, Göttingen, Germany, **1997**.

17 G. Rombaut, S. Golhen, L. Ouahab, C. Mathoniére, O. Kahn, *J. Chem. Soc., Dalton Trans.* **2000**, 3609.

18 D. M. L. Goodgame, H. El Mkami, G. H. Smith, J. P. Zhao, E. J. L. McInnes, *Dalton Trans.* **2003**, 34.

19 S. Naskar, D. Mishra, S. K. Chattopadhyay, M. Corbella, A. J. Blake, *Dalton Trans.* **2005**, 2428.

20 C. Duboc, T. Phoeung, S. Zein, J. Pécaut, M.-N. Collomb, F. Neese, *Inorg. Chem.* **2007**, *46*, 4905.